# Kinetics vs. Thermodynamics: walking on the line for a five-fold increase in MnSi Curie Temperature.

Adrián Benedit-Cárdenas[a], Stéphanie Bruyère[a], Sylvie Migot[a], Thomas Hauet[a], Sébastien Petit-Watelot[a], Pascal Boulet[a], Dominique Muller[c], Dmitry A. Zuev[b], David Horwat[a] and Alexandre Nominé[a,d]

[a.] *Institut Jean Lamour, UMR CNRS 7198, Université de Lorraine, BP 70239, F-54506, Vandœuvre-lès-Nancy, France*
[b.] *Department of Nanophotonics and Metamaterials, ITMO University, St. Petersburg, 197101, Russia.*
[c.] *ICube laboratory (Université de Strasbourg and CNRS), 23 rue du Loess, BP 20 CR, F-67037 Strasbourg Cedex 2, France*
[d.] *Jozef Stefan Institute, Jamova Cesta 39, Ljubljana, EU SI-1000, Slovenia*

# Supplementary material

## Predicting composition model

During sputtering a voltage difference is stablished between the cathode and the anode inside the chamber. Even if the electrodes are not in contact, an electrical current is also stablished through the gas phase as a plasma is generated. Inside the chamber the current comes from the movement of electron to the anode and the sputtering gas (in this case argon) ions to the cathode. The current applied to the target is related to the sputtering gas dynamic. Taking into account the current continuity between inside and outside the chamber and neglecting the influence of secondary electron emission yield, the number of Argon ions striking a target during a time unit is equal to the current applied to target divided by the elemental charge. That is:

$$\frac{\#\ of\ Ar\ ions}{t} = \frac{I}{e} \qquad (1)$$

Where $I$ is the current applied to target and $e$ is the elemental charge. The number of sputtered atoms depends on the quantity of striking sputtering ions and the sputtering yield as is shown in equation 2. At the same time, the sputtering yield depends directly on the material of the target and the applied voltage. In equation 2, $N_{sput}$ is the number of sputtered atoms and $Y_{target}(V)$ voltage depending sputtering yield of the target's material.

$$N_{sput} = \#\ of\ Ar\ ions * Y_{target}(V) \qquad (2)$$

In terms of amount of substance and fluence, equation can be written as:

$$\dot{n}_{sput} = \frac{\#\ of\ Ar\ ions}{tN_0} Y_{target}(V) \qquad (3)$$

Where $\dot{n}_{sput}$ is the amount of substance sputtered from the target per time's unit, that is the sputtering rate; while $t$ and $N_0$ are the time's unit and Avogadro's number respectively. It is assumed that the relation between the sputtering rate and the deposition rate is linear. That is:

$$\dot{n}_{dep} = C * \dot{n}_{sput} \qquad (4)$$

Where $\dot{n}_{dep}$ is the deposition rate and $C$ is the constant of proportionality that depends mostly on the probability of collision of the sputtered atom during its drift between the target and the film surface. Equations 5 and 6 are obtained from the combination of equations 1, 3 and 4 applied to each to both manganese and silicon targets respectively.

$$\dot{n}_{Mn\,dep} = C_{Mn}\frac{I_{Mn}}{eN_0}Y_{Mn}(V_{Mn}) \qquad (5)$$

$$\dot{n}_{Si\,dep} = C_{Si}\frac{I_{Si}}{eN_0}Y_{Si}(V_{Si}) \qquad (6)$$

In equations 5 and 6 $\dot{n}_{Mn\,dep}$ and $\dot{n}_{Si\,dep}$ are the deposition rates; $I_{Mn}$ and $I_{Si}$ are the current for targets; $Y_{Mn}$ and $Y_{Si}$ are the sputtering yields; $V_{Mn}$ and $V_{Si}$ the applied voltage; and $C_{Mn}$ and $C_{Si}$ are the constant of proportionality between sputtered and deposited atoms of manganese and silicon, respectively. In the specific case of this work the working pressure during sputtering was around 0.39 Pa, which is a relatively low pressure for sputtering. Under these conditions, the effect of collision is considered small. Only a small portion of the sputtered atoms are prevented from arriving at the film. Then, since the major source of difference between $C_{Mn}$ and $C_{Si}$ is small, it is considered that these constants are equal.

$$C_{Mn} = C_{Si} \qquad (7)$$

The sputtering yield dependence on the voltage has been already reported and was used as input in this model. The ratio between the atomic deposited amounts of manganese and silicon is obtained by dividing equation 5 and 6. This relation is shown in equation 8 and take into account the assumption 7 . The ratio of composition $R$ depends on the current at the targets and their sputtering Yield. As mentioned before, the sputtering yield depends directly on the applied voltage. Moreover, if the sputtering process is being controlled by current, as is the case, then the voltage depends on the current through the $IvsV$ curve that has to be measured.

$$R = \frac{\dot{n}_{Mn\,dep}}{\dot{n}_{Si\,dep}} = \frac{I_{Mn} * Y_{Mn}(V_{Mn})}{I_{Si} * Y_{Si}(V_{Si})} \qquad (8)$$

Equation 8 is used to predict the setup current at the targets for deposit a film with the desired composition. The measured $IvsV$ curve and the reported sputtering yield dependence on voltage were used as input data.

## Composition

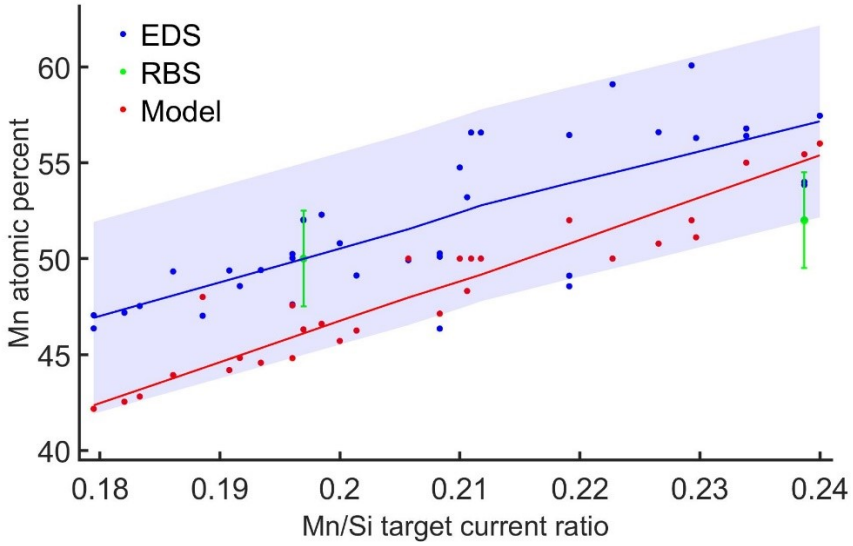


*Figure S 1. film composition calculated for different sputtering currents setup. The composition values are measured by EDS and RBS, and predicted by the setup model. The red line is a smoothing of model prediction values. The blue line is a smoothing of the experimental EDS data and the blue band the corresponding uncertainty range (5%). The uncertainty of RBS value is 2.5%.*

## Magnetic inspection

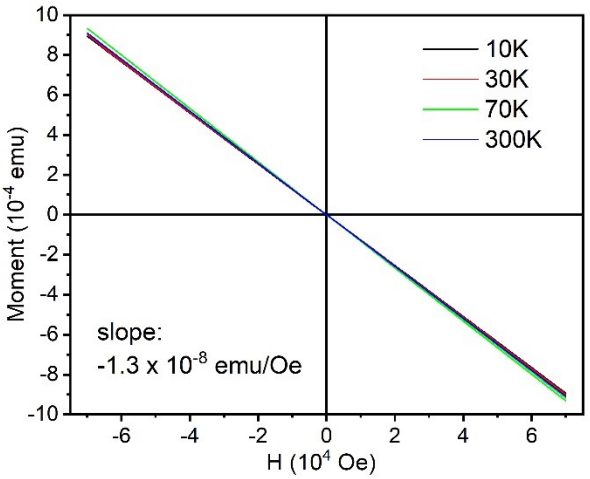


*Figure S 2. Diamagnetic response from the sapphire substrate. The slope of the moment with respect to the magnetic field is clearly negative. This negative slope signal was removed from the moment curves of all samples. The measure was made at*

*different temperatures and the slope's value doesn't change considerably. The external magnetic field was applied parallel to the substrate*

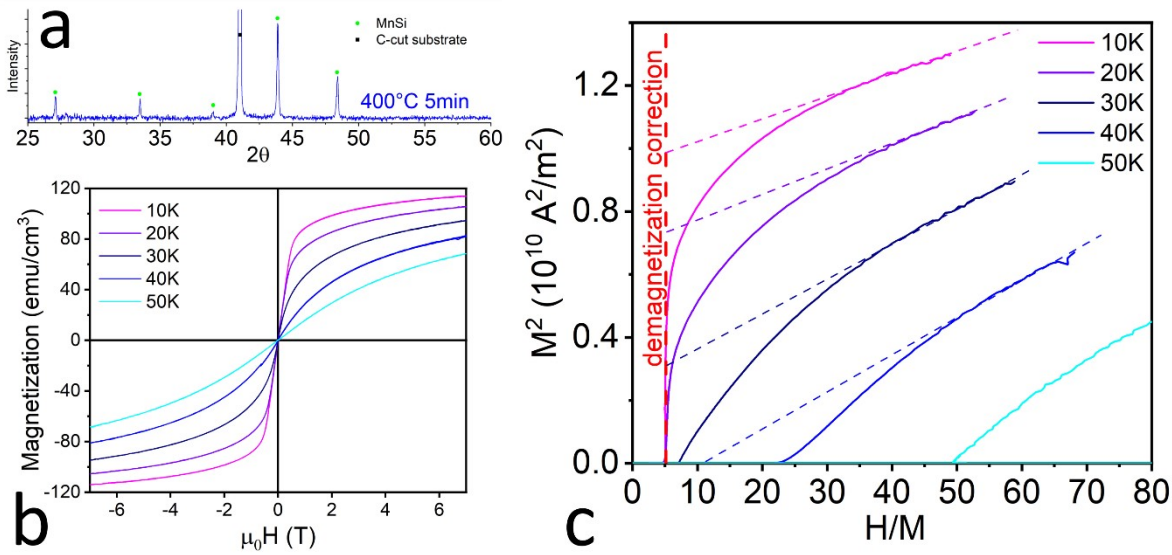


*Figure S 3. Single MnSi phase reference film. Diffractogram in **a** shows the single phase film's character, all the peaks, besides the substrate's peak, correspond to MnSi cubic phase. The M vs H cycles at different temperatures is represented in **b**. The reference film does not show remanence. The Curie temperature was calculated by the Arrott's plot which is shown in **c**. M evolve linearly with H at low field and temperatures as can be noted in **b**. The end of the linearity in each isotherms mark the demagnetizing field value. The Arrott's plot of a corresponding linear fit is represented by the discontinuous red line in **c**, where H stand for external magnetic field. The internal magnetic field can be obtained by removing the demagnetizing magnetic field which means relocate the zero-field point at the position of the red line in **c**. The high field linear extrapolation intercepting the red line in **c**, indicates a ferromagnetic state while intercepting H/M axis indicates a paramagnetic state. According to **c**, the Curie temperature lies between 30K and 40K.*

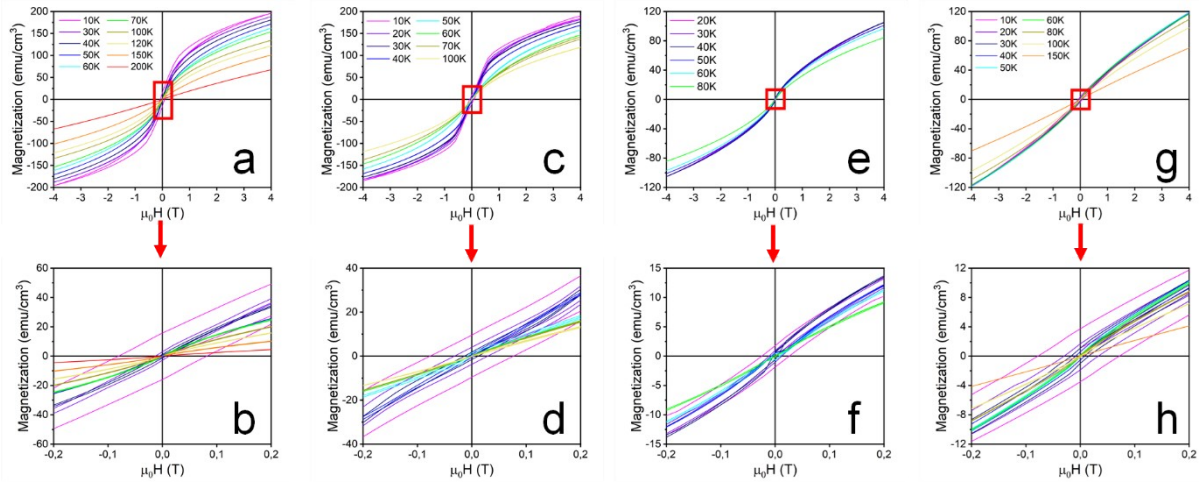


*Figure S 4. Magnetic behaviour. M vs H cycles of films with starting 52 Mn at. % composition and annealed at 600°C for 5 minutes and 800°C for 9 seconds are shown in **a** and **c** respectively. Films with starting 54 and 56 Mn at. % (both annealed at 400°C for 5 minutes) are shown in **e** and **g** respectively. Cycles in **b**, **d**, **f** and **h** correspond to a zoom on the area defined by the red square, at the origin of coordinates, of cycles **a**, **c**, **e** and **g**, to check remanence.*

# Microstructure

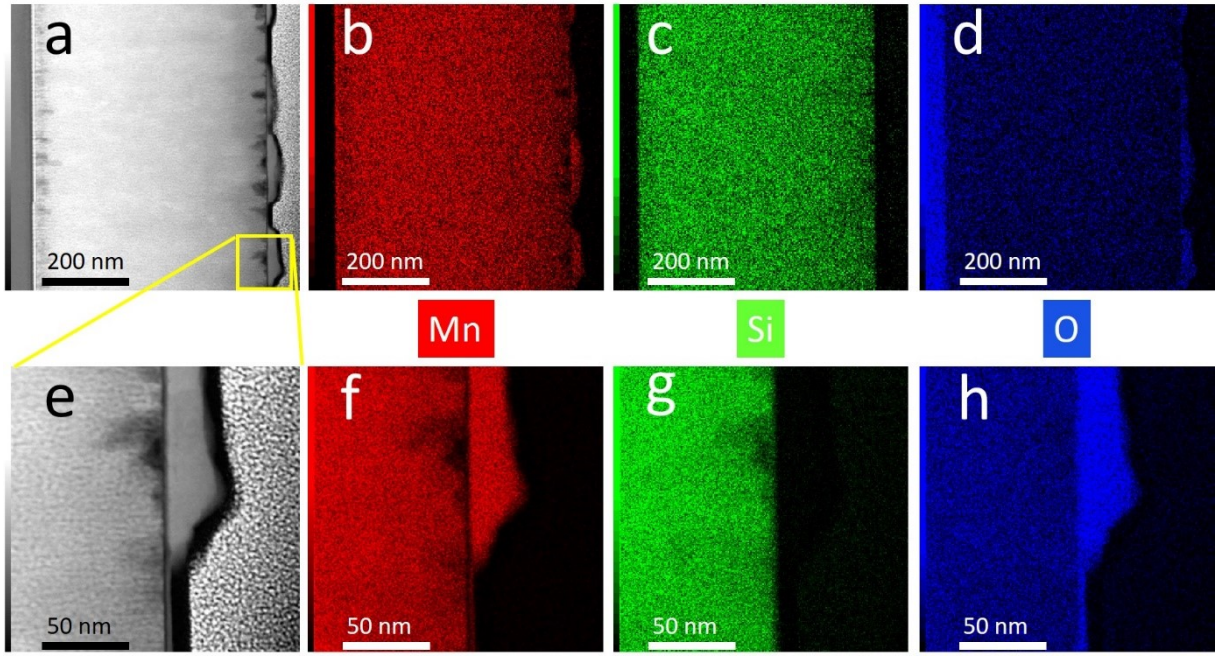


*Figure S 5. Scanning transmission electron microscopy (STEM) on films annealed at 400°C. Several islands appear on the top of the film as can be seen in the dark field image **a**. The islands are constituted by manganese oxide as can be deducted from the corresponding Mn, Si and O EDS cartographies shown in **b**, **c** and **d**; respectively. STEM dark field image **e** is a zoom on one of the islands in **a**, while **f**, **g** and **h** are the corresponding Mn, Si and O EDS cartographies respectively.*

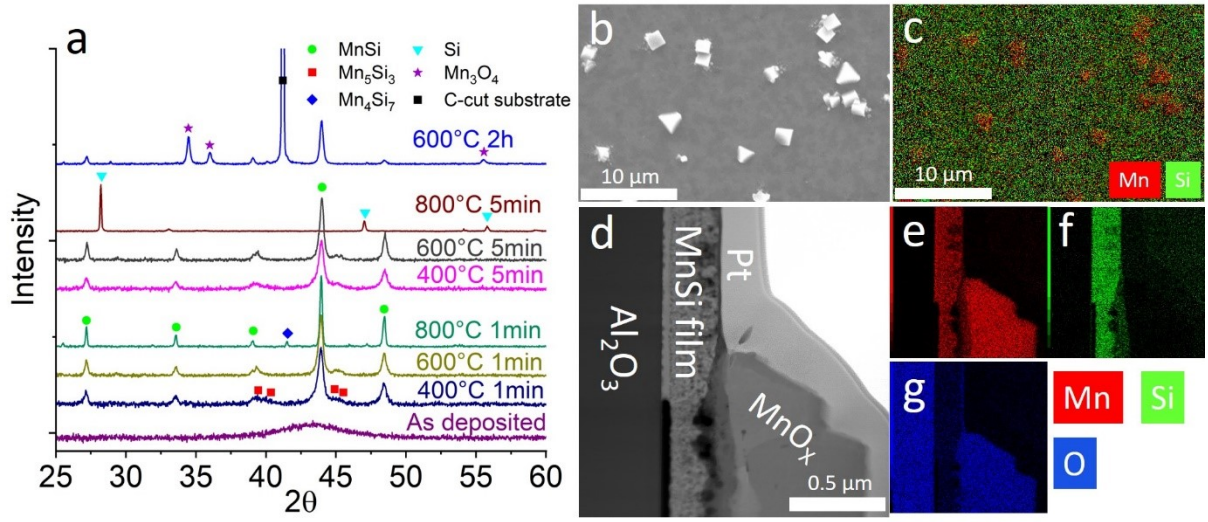


*Figure S 6. The diffractograms from films annealed for 1 and 5 minutes at 400°C, 600°C and 800°C and film annealed at 600°C for 2 hours are shown in **a**. Manganese oxide island can be detected on the top of film annealed at 600°C for 2 hours in the SEM image **b** and the corresponding EDS cartography **c**. One of these islands appear in the STEM dark field image **d**, as well as, the corresponding Mn, Si and O EDS cartographies shown in **e**, **f** and **g**; respectively.*

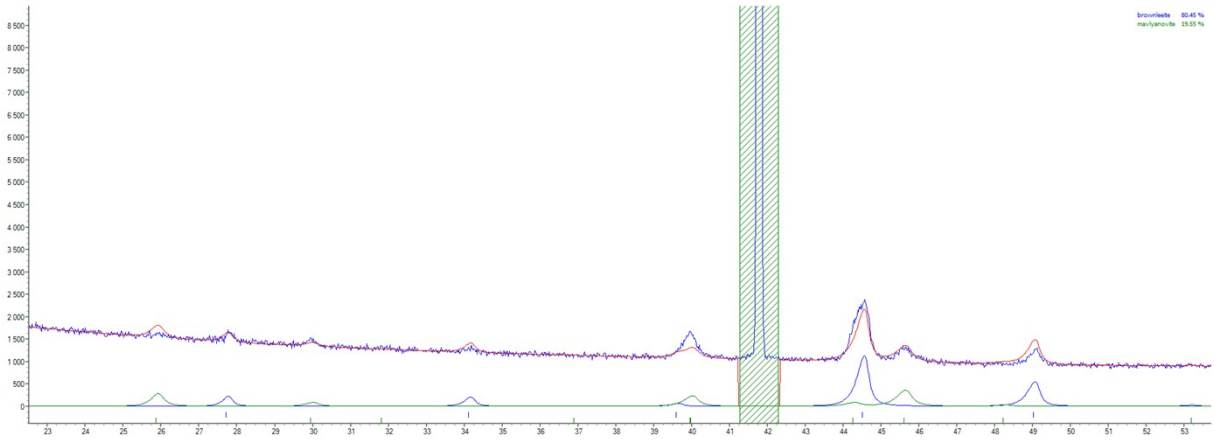


*Figure S 7. Rietveld type refinement obtained for one sample, with in blue the experimental diagram, in red the theoretical one and in blue and green the theoretical pattern of MnSi and $Mn_5Si_3$ respectively. The green hatched part corresponds to the sapphire substrate contribution which was not taken into account for the refinement. The refinement was performed for each sample, with the program TOPAS (Bruker AXS) using the instrument function approach.*

*6 polynomial parameters for background, one for the sample displacement, 2 for the scale factor of each phase, and 3 for the unit cell dimensions of MnSi (Cubic) and $Mn_5Si_3$ (hexagonal). The structure factors were calculated using the CIF files obtained from https://doi.org/10.1107/S1600576716006282 and https://doi.org/10.1039/C2JM00154C for MnSi and $Mn_5Si_3$ respectively.*

*The reliability factor obtained for this refinement is Rwp = 4.8% leading to the lattice parameters a = 4.548(7) Å for MnSi and a = 6.88(1) Å and c = 4.869(8) Å for $Mn_5Si_3$.*